Substantiation of buried two dimensional hole gas (2DHG) existence in GaN-on-Si epitaxial heterostructure

Jinming Sun, Giorgia Longobardi, Florin Udrea, Congyong Zhu, Gianluca Camuso, Shu Yang, Reenu Garg, Mohamed Imam, and Alain Charles

Citation: Appl. Phys. Lett. **110**, 163506 (2017); doi: 10.1063/1.4980140
View online: http://dx.doi.org/10.1063/1.4980140
View Table of Contents: http://aip.scitation.org/toc/apl/110/16
Published by the American Institute of Physics

Substantiation of buried two dimensional hole gas (2DHG) existence in GaN-on-Si epitaxial heterostructure

Jinming Sun,[1] Giorgia Longobardi,[2] Florin Udrea,[2] Congyong Zhu,[1] Gianluca Camuso,[2] Shu Yang,[2] Reenu Garg,[1] Mohamed Imam,[1] and Alain Charles[1]
[1]*Infineon Technologies Americas Corp, El Segundo, California 90245, USA*
[2]*Cambridge University, Cambridge CB30FA, United kingdom*

(Received 7 December 2016; accepted 3 April 2017; published online 20 April 2017)

Gallium Nitride on Silicon (GaN-on-Si) devices feature a relatively thick epi buffer layer to release the stress related to the lattice constant mismatch between GaN and Si. The buffer layer is formed by several AlGaN-based transition layers with different Al contents. This work addresses the fundamental question of whether two-dimensional hole gases (2DHGs) exist at those interfaces where the theory predicts a high concentration of a negative fixed charge as a consequence of the discontinuity in polarization between the layers. In this study, we demonstrate that the presence of such 2DHGs is consistent with the measured vertical Capacitance-Votage Profiling (CV) and Technology Caomputer-Aided Design (TCAD) simulation in the whole range of measurable frequencies (10 mHz–1 MHz). N-type compensating background donor included in the epi structure in the simulation deck proves to be crucial to explain the depletion region extension consistent with the CV experimental data. For the standard range of frequencies (1 kHz–1 MHz), there was no indication of the presence of 2DHGs. A set of ultra-low frequency (10 mHz–10 Hz) measurements performed were able to reveal the existence of 2DHGs. The outcome of these ultra-low frequency experiments was matched with TCAD simulations which validated our theory. *Published by AIP Publishing*. [http://dx.doi.org/10.1063/1.4980140]

GaN-based power devices have been recognized as the most promising technology able to displace Si in 600 V-rated power applications for achieving high efficiency energy conversion. This is due to the unique material advantage of GaN over its Si counterpart, such as the high critical electric field (3.3 MV/cm) and high channel mobility (~2000 cm^2/Vs) of electrons confined in the channel at the AlGaN/GaN interface.[1–5] Moreover, the possibility to grow GaN on the Si substrate has paved the way to a low-cost, high efficient gallium nitride on silicon (GaN-on-Si) technology. However, epi growth-related problems, such as defects and dopants behaving as traps, lead to reliability issues and thus constitute a challenge to the optimum performance of these technologies.[6,7] In order to solve trap-related malfunctions, it is essential to understand the interplay between carriers, traps, and transport processes through various interfaces.[8] An effective way to do this is to build a realistic Technology Caomputer-Aided Design (TCAD) model able to take into account the various transport mechanisms and trap dynamics. The endeavor to model the epi layer of GaN-on-Si is baffled by the unknowns inside the epi at the present time. Due to the lattice constant mismatch between (111) Si and (0001) GaN, the stress management of the film often dictates a multi-layer epi growth scheme with layers of $Al_xGa_{1-x}N$ of descending x from bottom to top. Such arrangement evokes a fundamental question regarding the existence of Two Dimensional Hole Gas (2DHG) present at these interfaces generated by the high negative polarization charge.

The question is of paramount importance for any serious attempt to model the epi stack, since the presence or the lack thereof of these carriers affect the carrier modulation of the field and a host of transient/dynamic charging phenomena. This is because if 2DHGs are present, for the same high voltage applied, the depletion region in the buffer and transition layers will be reduced, thus increasing the vertical capacitance level. Very few reports on the detection of 2DHG were published[9–12] and even fewer on 2DHG within the transition layer stack.[13] In Refs. 9–12, the 2DHGs discussed are electrically connected to the source and drain contacts, thus behaving as conductive channels (and not buried in the epi-structure or transition layer as discussed in this manuscript). This allowed the detection and characterisation of 2DHG concentration by means of conventional electrical characterisation by measuring the channel conduction current. In addition, many of these analyzed structures include a heavily Mg doped p-type cap, making the origin of the 2DHG fuzzy. In those publications where the 2DHG at transition layers' interface is the focus of study,[13] variable magnetic fields and temperature Hall effect measurements together with the mobility spectrum analysis (i-QMSA) were employed to detangle the contribution of 2DHG from the one given by the 2DEG within the channel. The conclusion whether 2DHG exists at the interface or not was far from being obvious. Due to this very uncertainty about 2DHG, many theoretical and simulation works have adopted the approach to treat the multi-layered epi with a simplified composition of layers or more often to lump them into a single layer, avoiding the issue of 2DHG at the interfaces altogether.[7,8,14,15] We have also carried out extensive Capacitance-Votage Profiling (CV) measurements in the standard frequency range (kHz to MHz), but no convincing evidence of the existence of the hole carrier layer has been found. In this work, the authors demonstrate via measurements and TCAD simulations that an ultra-low frequency CV is a key to the detection of the 2DHG in the epi stack. No detection of 2DHG in this manner has ever been reported.

Fig. 1(a) shows the MOCVD-grown GaN-on-Si epi structure, as measured and simulated. The epitaxial growth

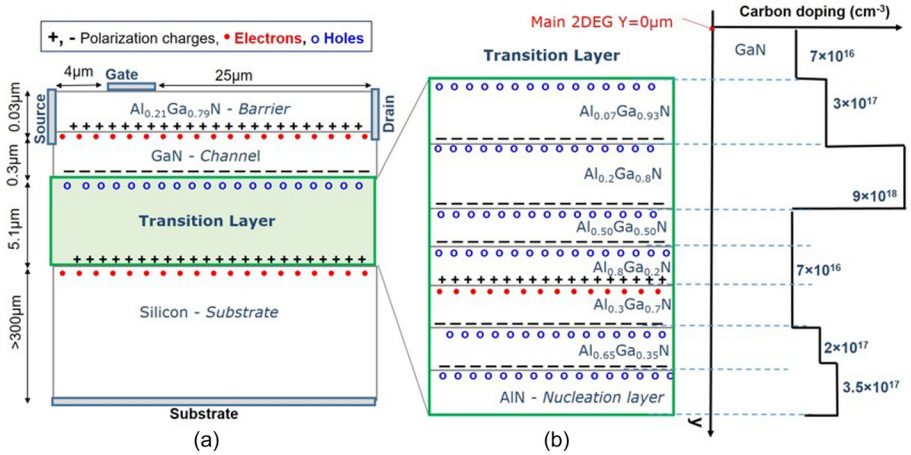

FIG. 1. (a) The representative epi structure of GaN on Si using the multi-transition layer growth scheme. On a light p Si substrate, $Al_xGa_{1-x}N$ layers of descending mole fraction x have been grown on top of each other. At various interfaces, 2DEG and 2DHG are shown in the figure. The corresponding net polarization charge (positive and negative) is also shown. (b) Carbon doping profile as included in the epi-structure.

begins with a nucleation layer of AlN on a p-doped silicon substrate. Due to the lattice constant mismatch between silicon (111) and GaN (0001), a multi-layer scheme with descending mole fraction (Transition Layer) is employed between the nucleation layer and the GaN channel to manage the growth stress. The main 2DEG (i.e., the channel of the transistor) is formed at the interface between the AlGaN barrier layer and the GaN channel layer at $y = 0\,\mu m$. Typical dimensions of the active layer and the transition layer together with the used Al mole fractions are given in Fig. 1(a). The III-nitride material is a pyroelectric material with a negative polarization (pointing down) for the Ga-face growth, which increases linearly with the Al mole fraction x.[16] As a consequence, at the interface between an upper layer with a given x value and an under layer with a lower x value, a net positive charge exists, such as at the interface between the AlGaN barrier and the GaN channel, resulting in the generation of the 2DEG. Similarly, at the interface between an upper layer with a low x value and an under layer with a high x value, as it is the case for all the interfaces in the transition layers, a net negative charge exists. As a result of this very high negative fixed charge, a 2DHG should be formed at each of these interfaces based on electrostatics ground. Carbon doping was included in the epi-structure in order to reduce the off-state leakage. The doping profile extracted from SIMS measurements is schematically reproduced in Fig. 1(b).Vertical CV measurements and numerical simulations were carried out on the structure of Fig. 1(a).

In order to perform this analysis, source, drain, and gate electrodes were connected together to a zero bias terminal, and a negative sweeping voltage was applied to the substrate. With this configuration, the main 2DEG that is electrically connected to the zero potential via the source and drain contacts behaves as the "top plate" of the measured CV, while the substrate acts as the "bottom plate." The measured and simulated CV characteristic refers to the capacitance between the top and bottom plate as a function of the increasing voltage $= V_{top}$-V_{bottom}. For ultra-low frequencies, the maximum limit imposed by the system is 20 V. The sweep rate is dependent on the measurement frequency with 10 V/s for $f = 1$ kHz and with 1 mV/s for $f = 10$ mHz. The Synopsys TCAD software was used to simulate the structure in Fig. 1(a) and confirm the experimental analysis. The drift diffusion model is employed, and nominal GaN material parameters are used unless otherwise specified. Unlike many simulation works which simplify or lump the transition layers together, polarization charge at all interfaces are calculated and placed according to Refs. 16 and 17. All the layers simulated, except the top AlGaN barrier, are assumed to be completely relaxed. A surface donor trap of $2.7 \times 10^{13}\,cm^{-2}$ and $E_t = 0.18$ eV from the conduction band is placed at the surface of the AlGaN barrier.[14] The epi bulk acceptor trap spatial distribution are modeled according to the carbon profiling as shown in Fig. 1(b) with an energy level equal to 1.3 eV above the valence band. This energy level, deeper than the commonly quoted 0.9 eV for carbon,[18] is chosen. The comparison between the effects of these two levels, however, is considered and included in the following analysis. An N-type background doping equal to $9 \times 10^{14}\,cm^{-3}$ was included in the simulated epi, and its influence on the CV is discussed in details with the results.

Figure 2 shows the simulated band diagram (a) and electron/hole concentration (b) in the epi at zero bias. The several peaks of hole concentration referred as 2DHGs and confined at the interfaces wherever negative net polarization charge resides are clearly indicated. The measured and simulated vertical CV curves at $f = 1$ kHz are shown in Fig. 3. One can note that the simulations with carbon level 1.3 eV predict fairly well the experimental results with the capacitance being equal to $\sim 1.7\,nF/cm^2$ at zero bias and stepping down to $\sim 1.33\,nF/cm^2$ at $V = \sim 370$ V. The step observed in the CV is associated with the depletion of the main 2DEG-channel which acted as the top plate of the capacitance and as such was shielding the contribution to the CV given by the layers above it. Once the 2DEG is depleted, the capacitance of the top layers (above 2DEG) contributes to the series of the capacitance (below the 2DEG), leading to a reduction in the overall vertical capacitance.

The depletion of the 2DEG with the voltage is clearly shown in the inset of Fig. 3 where a negligible 2DEG density is observed for $V > 250$ V voltages for which the CV drops to its lower value.

It is clear from the comparison of the simulated results in Fig. 3 that modeling the carbon as a single acceptor at 0.9 eV leads to a disagreement with the measurement results in two significant ways: (1) a step is observable around 90 V for $f = 1$ kHz for the depletion of the 2nd 2DHG and (2) the

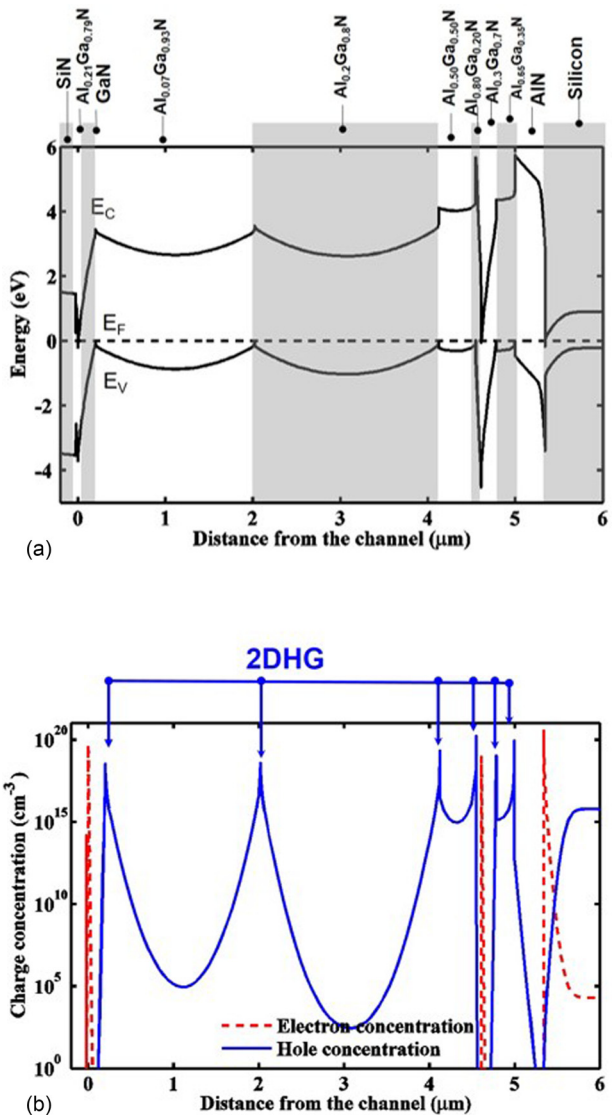

FIG. 2. (a) Conduction band, valence band, and Fermi level at equilibrium. (b) Electron and hole density at equilibrium.

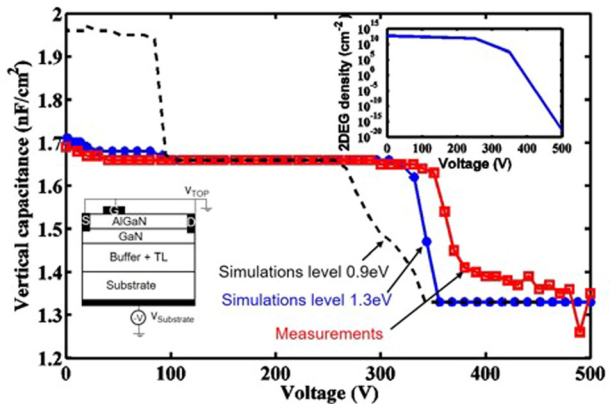

FIG. 3. Measured and simulated vertical CV of a device with the epi stack is shown in Fig. 1 at f = 1 kHz. The simulated curves are for carbon levels of 1.3 eV and 0.9 eV from the valence band, showing a much better match for the deeper level 1.3 eV. The steps in the CV around 350 V correspond to the depletion of the 2DEG channel (Inset-top-right). CV measurement and simulation electrical connections (Inset-bottom-left).

step corresponding to a faster depletion of 2DEG appears at lower voltage. The fact that both effects are absent in the real measurement indicates that the heavily doped carbon, to a large extent, remains inactive in creating p carriers and in trapping, possibly through a self-cancelling arrangement such as in the model of autocompensation.[7] Its role in 2DHG detection thus is very limited, and for this reason, a deeper trap energy level (1.3 eV) was considered for it. In fact, TCAD simulations predicted that even in the absence of the carbon acceptor traps the major conclusions regarding 2DHG at normal and ultralow frequency still hold.

In order to match the experimental results, n-type background doping of $9 \times 10^{14}\,cm^{-3}$ was included in the TCAD input deck. Neglecting the presence of such background doping would result in a very high hole concentration in between the 2DHGs present in the transition layer, as shown in the inset of Fig. 4. While the 2DHG peak densities at the interfaces remain practically unaffected, the bulk hole density inside the regions connecting the different 2DHGs has been reduced by ten orders of magnitude with the introduction of the compensating donor doping. In fact, the RC response time of the 2DHGs to the AC signal without the background doping reduces significantly. The uncompensated epi would therefore reveal the presence of the 2DHGs in a series of steps corresponding to the consecutive depletion of them.

This is shown in Fig. 4 where the simulated CV is plotted with and without the n-type background doping. It is worth mentioning that n-type background doping is known to be present in MOCVD grown GaN epi by virtue of oxygen impurities acting as donors.[17] We believe that considering the n-type compensation is crucial to reproduce the charge balance inside the overly p-type epi, and at the same time, it is the main factor that suppressed the 2DHGs signal from being seen in our CV experiments in the normal frequency range (kHz to MHz). In Fig. 5, the simulated CV without 2DHGs (obtained by removing the negative polarization charge at the heterointerfaces) is shown. The CV curve in this case is flat at a low voltage range, a characteristics shared by the measured CV as well as simulated CV with 2DHG compensated by background compensating donors at f = 1 kHz. One can also notice that the 2DEG depletion occurs at much higher voltages in the case of no 2DHGs in the epi-structure.

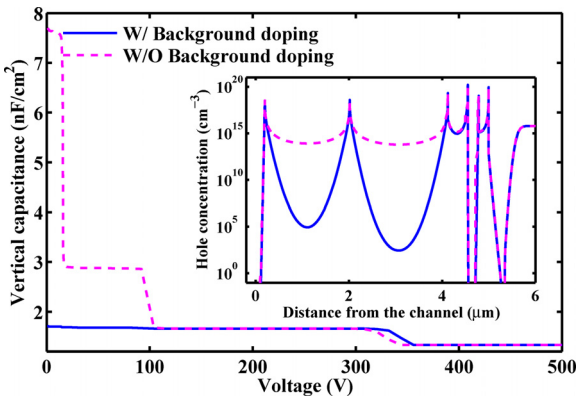

FIG. 4. Simulated vertical CV at f = 1 kHz with $9 \times 10^{14}\,cm^{-3}$ of n-type background doping and without background doping. Inset: Simulated hole density without and with background compensating donor of $9 \times 10^{14}\,cm^{-3}$ at zero bias.

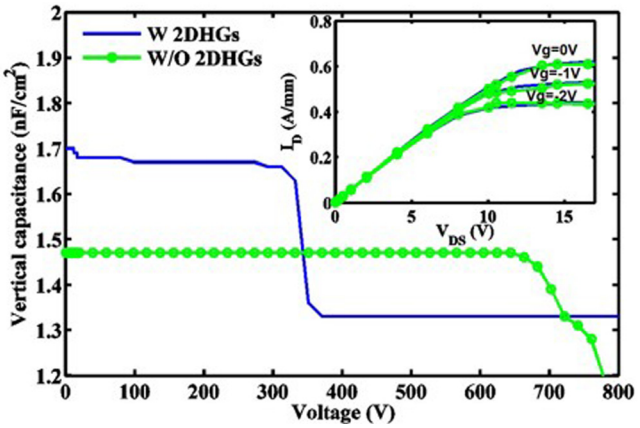

FIG. 5. Simulated CV at f = 1 kHz with and without 2DHGs (background n-type doping 9×10^{14} cm^{-3} and carbon energy level 1.3 eV from the valence band). Inset: IdVd with and without 2DHGs.

An ultralow frequency CV experiment was set in order to capture the slow response of the 2DHGs in a compensated epi to the AC signal. This was followed by an equivalent simulation set-up. The results of this analysis are shown in Fig. 6 where it can be observed that the measurement reveals a significant transition step, corresponding 2DHG push-out by the positive bias, at 10 mHz. This is in strong agreement with the simulation result. The step size as well as the zero-volt-capacitance value decreases with increasing frequency and eventually transitions to a flat CV at a high frequency. Although quantitative match is not perfect at this point, the qualitative agreement between simulation and experiment strongly supports the existence of 2DHG at the interfaces between epi layers. Given the different growth condition for each layer of the epi-structure, it is conceivable that the spatially uniform compensating donor profile is a simple but not realistic representation of the background doping profile. This could be a potential cause of quantitative difference in Fig. 6. The precise profile is unknown in the literature. It is very likely to depend on growth conditions, Al mole fraction, and P-type doping. One theory of compensation involves carbon.[7]

It is important to stress that the ultralow frequency (10 mHz to 10 Hz) CV admittance was verified to be dominated

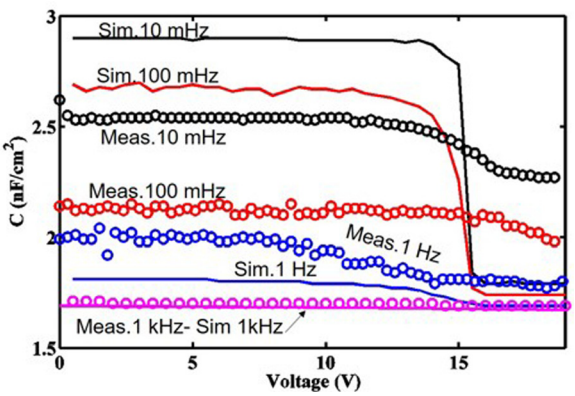

FIG. 6. Simulated and measured ultralow frequency (10 mHz, 100 mHz, and 1 Hz) and high frequency (1 kHz) vertical CV measurement. At 10 mHz, a step of considerable size around 15 V is clearly observable in both simulation and measurement. The step size and the capacitance at zero volt decrease with increasing frequency and becomes virtually flat for f > 10 Hz.

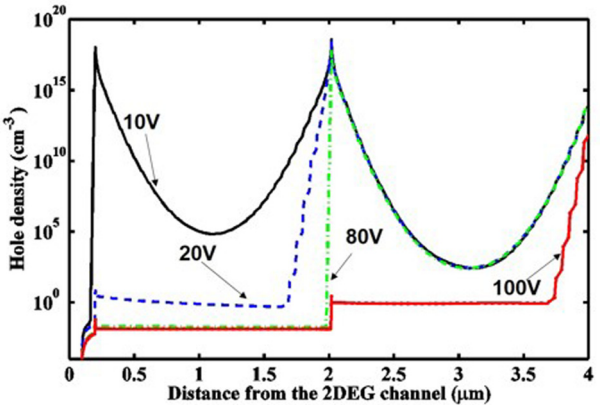

FIG. 7. Simulated hole density during the CV sweep at 10 mHz for V = 10, 20, 80, and 100 V.

by capacitance (phase angle close to 90°). Moreover, to further confirm the dominance of the capacitive contribution over a change in the vertical resistance in the ultralow frequency capacitance, quasi-DC vertical leakage current was measured for the same range of voltages (up to 20 V). Unfortunately, the measured current is in the range of pA, close to instrument detection limit and cannot provide any relevant information.

Fig. 7 shows the depletion of the top two 2DHG corresponding to the step at ~15 and 90 V (not shown due to the limitation of the experimental set-up). The good match of the step voltage between measurements and simulations (Fig.6) is an indication that the value of interface charge considered in our analysis is realistic. We expect that a reduction in interface charge would result in a variation in the voltage at which the step occurs but not at the capacitance level. A shift in the voltage step (in measurements seen at ~15 V) can only occur when the 1st interface charge (corresponding to the 1st most-shallow-2DHG) varies. For a fixed 1st interface charge, a 2nd interface charge (corresponding to the 2nd 2DHG from the top) variation produces no shift of the step because of the shielding created by the first 2DHG. This can be clearly seen from the simulation results shown in Fig. 8 where the capacitance is plotted against the voltage for different levels of 1st and 2nd interface charges.

We have demonstrated that the presence of 2DHGs is consistent with the measured vertical CV and TCAD

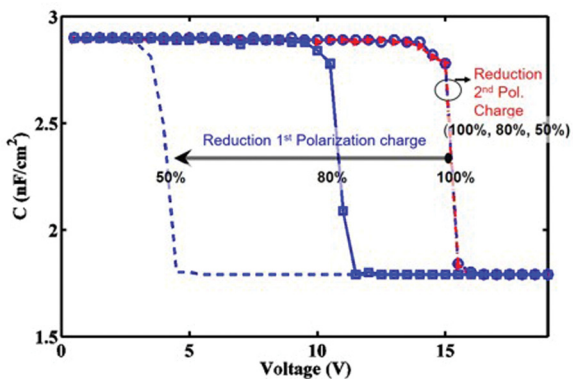

FIG. 8. Simulated f = 10 mHz CV with variation of 1st and 2nd interface charge from 100% to 50% showing the sensitivity of the step at 15 V to the 1st interface charge but not to the 2nd.

simulation in the whole range of measurable frequencies (10 mHz– 1 MHz). Compensating background donor inside the epi is the a key factor in the suppression of the high frequency CV steps corresponding to 2DHG depletion. Although background doping has been previously included in simulation decks,[18] this is the first time that its impact on the vertical CV is discussed, and moreover, this is the first time that the 2DHG has been detected using an ultralow frequency CV measurement.

J. Sun wishes to thank G. Curatola for valuable insight, S. Khalil for helpful input, Device Characterization team at Chandler AZ, and Epi development team at Mesa AZ of Infineon Technologies Americas for characterization support and sample supply.

[1]M. J. Uren, M. Casar, M. Gajda, and M. Kuball, Appl. Phys. Lett. **104**, 263505 (2014).
[2]B. Lu and T. Palacios, IEEE Electron Device Lett. **31**, 951–953 (2010).
[3]M. Meneghini, C. de Santi, T. Ueda, T. Tanaka, D. Ueda, E. Zanoni, and G. Meneghesso, IEEE Electron Device Lett. **33**, 375–377 (2012).
[4]W. Saito, M. Kuraguchi, Y. Takada, K. Tsuda, I. Omura, and T. Ogura, IEEE Trans. Electron Device **52**, 106–111 (2005).
[5]B. Lu, O. I. Saadat, and T. Palacios, IEEE Electron Device Lett. **31**, 990–992 (2010).
[6]P. B. Klein, S. C. Binari, K. Ikossi, A. E. Wickenden, D. D. Koleske, and R. L. Henry, Appl. Phys. Lett. **79**, 3527–3529 (2001).
[7]A. Chini, G. Meneghesso, M. Meneghini, F. Fantini, G. Verzellesi, A. Patti, and F. Iucolano, IEEE Trans. Electron Device **63**, 3473–3477 (2016).
[8]D. Cornigli, S. Reggiani, E. Gnani, A. Gnudi, G. Baccarani, P. Moens, P. Vanmeerbeek, A. Banerjee, and G. Meneghesso, in IEDM Technical Digest (2015), p. s5p3.
[9]A. Nakajima, Y. Sumida, M. H. Dhyani, H. Kawai, and E. M. Sankara Narayanan, Appl. Phys. Express **3**, 121004 (2010).
[10]T. Zimmermann, M. Neuburger, K. Kunze, I. Daumiller, A. Denisenko, A. Dadgar, A. Krost, and K. Kohn, IEEE Electron Device Lett. **25**, 450–452 (2004).
[11]S. Hackenbuchner, J. A. Majewski, G. Zandler, and P. Vogl, J. Cryst. Growth **230**, 607–610 (2001).
[12]H. Hahn, B. Reuters, A. Pooth, B. Hollander, M. Heuken, H. Kalisch, and A. Vescan, IEEE Trans. Electron Device **60**, 3005–3011 (2013).
[13]S. Acar, S. B. Lisevivdin, M. Kasap, S. Ozcelik, and E. Ozbay, Thin Solid Films **516**, 2041–2044 (2008).
[14]M. Faqir, G. Verzellesi, A. Chini, F. Fantini, F. Danesin, G. Meneghesso, E. Zanoni, and C. Dua, IEEE Trans. on Device and Material Reliablity **8**, 240–247 (2008).
[15]D. Cornigli, F. Monti, F. Reggiani, E. Gnani, A. Gnudi, and E. Baccarani, Solid-State Electron **115**, 173–178 (2016).
[16]O. Ambacher, J. Smart, J. R. Shealy, N. G. Weimann, K. Chu, M. Murphy, W. J. Schaff, L. F. Eastman, R. Dimitrov, L. Wittmer *et al.*, J. Appl. Phys. **85**, 3222–3233 (1999).
[17]O. Ambacher, J. Phys. D: Appl. Phys. **31**, 2653–2710 (1998).
[18]M. J. Uren, J. Moereke, and M. Kuball, IEEE Trans. Electron Device **59**, 3327–3333 (2012).